Article

Not peer-reviewed version

Lipid Metabolism Reprogramming Is Associated with Trastuzumab Resistance in ERBB2+ Breast Cancer Cell Lines

Katia Cortese *, Marco Ponassi, Aldo Profumo, Gabriela Coronel Vargas, Erika Iervasi, Maria Cristina Gagliani, Grazia Bellese, Sara Tavella, Patrizio Castagnola *

Posted Date: 3 April 2023

doi: 10.20944/preprints202304.0002.v1

Keywords: trastuzumab; trastuzumab resistance; HER2; breast cancer; proteomic analysis; metabolic reprogramming.

Article

Lipid Metabolism Reprogramming Is Associated with Trastuzumab Resistance in ERBB2+ Breast Cancer Cell Lines

Katia Cortese [1], Marco Ponassi [2], Aldo Profumo [2], Gabriela Coronel Vargas [2,§], Erika Iervasi [2], Maria Cristina Gagliani [1], Grazia Bellese [1], Sara Tavella [2,3] and Patrizio Castagnola [2]

[1] DIMES, Department of Experimental Medicine, Cellular Electron Microscopy Lab, Università di Genova, Genova, Italy. cortesek@unige.it (KC), gagliani@unige.it (MCG), bgrazia@unige.it (GB), sara.tavella@unige.it (ST).

[2] IRCCS Ospedale Policlinico San Martino, Genova, Italy. marco.ponassi@hsanmartino.it (MP), aldo.profumo@hsanmartino.it (AP), erika.iervasi@hsanmartino.it (EI), sara.tavella@hsanmartino.it (ST). gabrielafernanda.coronelvargas@edu.unige.it (GCV).

[3] DIMES, Department of Experimental Medicine, Cellular Oncology Unit, Università di Genova, Genova, Italy.

* Correspondence: cortesek@unige.it (KC); patrizio.castagnola@hsanmartino.it **(PC)**

§ Present address: Department of Experimental Medicine, Università di Genova, Genova, Italy (GCV).

Simple Summary: Trastuzumab (Tz) is a monoclonal antibody, a molecule designed to exploit particular weaknesses in breast cancer cells. It works by recognizing the ERBB2 protein on cancer cells and stopping them from growing and reproducing. However, patients treated with Tz often become resistant to this therapy. Understanding the mechanisms underlying the onset of resistance would help developing better therapies and improve patients' lives. We used proteomic analysis, bioinformatic tools as well as ultramicroscopy to identify common features of breast cancer cells that are sensitive and resistant to Tz. We found 10 differentially expressed proteins (DEPs) in our breast cancer cell models that support the hypothesis that complex metabolic adaptations of the cells, including the reprogramming of lipid metabolism, may fuel Tz resistance. These proteins may be considered as novel targets for therapeutic intervention.

Abstract: The antibody Trastuzumab (Tz) targeting ERBB2 has improved the prognosis of patients with breast cancer (BCa) that overexpress this receptor. Resistance to Tz negatively impacts prognosis. Several mechanisms have been reported to cause Tz resistance. The objective of this study was to identify common mechanisms in in vitro models of acquired BCa Tz resistance. In particular, we used three widely available ERBB2+ BCa cell lines adapted to grow in Tz. We performed several analyses to address possible changes in phenotype, proliferation, and ERBB2 membrane expression common to the three Tz-R cell lines compared to wt, but none was found. High-resolution mass spectrometry analysis identified, instead, a common set of differentially expressed proteins (DEPs) in Tz-R vs. wt cells. Furthermore, bioinformatic tools revealed that all three Tz-R cell models shared a modulation of proteins involved in the metabolism of lipids, organophosphate biosynthetic process, and macromolecule methylation. Ultrastructural analysis confirmed alteration of lipid droplets in resistant cells. Our data strongly support the hypothesis that complex metabolic adaptation, including lipid metabolism, protein phosphorylation, and possibly chromatin remodeling, may fuel Tz resistance. The identification of a common set of 10 DEPs in all three TZ-resistant cell lines may provide novel targets for therapeutic intervention.

Keywords: trastuzumab; trastuzumab resistance; HER2; breast cancer; proteomic analysis; metabolic reprogramming

1. Introduction

Tumors overexpressing the ERBB2 receptor, a member of the EGFR/ERBB1 receptor family, are about 25% of all breast cancers (BCa) and are associated with poor prognosis since the disease has an

aggressive character and a high propension to metastasize [1,2]. Overexpression of ERBB2 causes overactivation of the MAPK/ERK and PI3 kinase/AKT pathways, which promote cell proliferation, differentiation, migration, and angiogenesis [3–5]. The introduction of the recombinant and humanized monoclonal antibody named trastuzumab (Tz), directed against the extracellular domain IV of ERBB2 in the therapy regimen significantly improved the patient's overall survival and disease-free survival [6,7]. Recently, novel Tz-based therapeutics have been developed, further reinforcing its crucial role in the management of ERBB2 BCa patients [8]. Tz impairs the survival of ERBB2 overexpressing cells and promotes antibody-dependent cell-mediated cytotoxicity [9,10]. Several mechanisms have been proposed to contribute to the Tz-induced inhibition of survival of ERBB2 overexpressing cells in vitro [11,12], which may partly dependent on the particular cell model used. Inhibition of ERBB2 growth signaling through the PI3K/AKT pathway [13] and accumulation of active CDKN1B in the nucleus leads to Cdk2 inactivation and arrest in the G0/G1 phase of the cell cycle is the most commonly acknowledged one [14]. Despite Tz effectiveness, about 35% of ERBB2+ breast cancer patients are de novo resistant to Tz and among those responsive, about 70% will eventually become resistant within one year of treatment [15]. Several molecular mechanisms have been proposed as responsible for Tz resistance [16]. These can be summarized into two broad categories: intrinsic to the cancer cells and extrinsic [e.g., host immune system-related]. Among the formers, the following may be included: [1] ERBB2 truncation, [2] impaired binding of Tz to HER2, [3] activation of compensatory or alternative signaling pathways, [4] defects in apoptosis and cell cycle control, [5] increased ability to generate cancer stem cells, [6] vascular mimicry and hypoxia, and [7] metabolic adaptation. Although extrinsic mechanisms may be of major relevance in naïve patients, it is conceivable that in patients receiving chemotherapy in the neoadjuvant setting, likely experiencing with time an immune-suppression state, intrinsic mechanisms of resistance may play a relevant role. We believe that despite limitation, an in vitro study may provide some insight into these intrinsic mechanisms. Using an unbiased approach, we aimed to reveal whether a cellular process could be associated with the development of acquired resistance to Tz in ERBB2+ BCa cell lines, with differences in receptor status [17] and sensitivity to Tz [18]. In particular, we used BT474, MDA-MB-361 and SKBR-3 wt and Tz-R cells that we adapted to grow in a Tz concentration about tenfold higher than therapeutic serum levels [19]. We investigated cell morphology, cell cycle, ERBB2 expression, and proteomic profile to identify possible molecular mechanisms at the bases of acquired Tz resistance shared by the three cell lines. Our results showed that proteins involved in metabolic reprogramming were differentially expressed by all the cell lines in the two conditions, which suggests that, at least in vitro, this process may contribute significantly to the development of cell-intrinsic Tz resistance.

2. Materials and Methods

Cell lines and cell culture reagents

The BC cell lines BT474, MDA-MD-361 and SKBR-3 were obtained from Banca Biologica and Cell Factory in IRCCS Ospedale Policlinico San Martino affiliated to the European Culture Collection's Organization. Culture media for routine cell expansion was DMEM high glucose supplemented with 1% glutamine, penicillin, streptomycin, and 10% heat-inactivated fetal bovine serum for BT474 and SKBR-3 or 20% for MDA-MD-361 (Euroclone S.p.A, Italy). To obtain Tz-R cells, each cell line was cultured and expanded in medium containing Tz at the initial concentration of 10 µg/ml that was progressively increased over about 6 months, to the final concentration of 160, 250, and 200 µg/ml for BT474, SKBR-3, and MDA-MD-361, respectively. Cells were routinely cultured in the Tz-containing medium for over a year before analysis. Tz was kindly provided by the pharmacy (UFA-Unità Farmaci Antiblastici) of the IRCCS Ospedale Policlinico San Martino.

Flow cytometry [FCM] analysis and antibodies.

To determine cell number, 50000 BT747 wt and Tz-R cells, 75000 MDA-MB-361 wt and Tz-R cells, and 35000 SKBR-3 wt and Tz-R cells were seeded per well in a corning 12 well plate (22.1 mm of

diameter) and the counts were performed after trypsinization by FCM. ERBB2 surface expression levels were investigated using Tz. A goat anti-human Alexa 647-conjugated antibody was used to detect Tz (Thermo Fisher Scientific, Waltham, MA). Cells were analyzed and counted using a CyFlow ML flow cytometer performing True Volumetric Absolute Cell Counting [TVAC] (Sysmex-Partec Inc., Lincolnshire, IL, USA) or a Cytoflex flow cytometer (Beckman Coulter, IN, USA).

Cell imaging

Phase-contrast images of sub confluent cell cultures were using an inverted Nexcope NIB620 microscope equipped with a peltier cooled FL-2 CCD camera (Bresser GmbH, Rhede, Germany).

Sample preparation, mass spectrometer setup and proteins identification.

Cell lines were cultured and treated in 75 cm^2 flasks. When treatment was completed, cells were washed twice in 1x PBS and then harvested by scraping. After centrifugation, cell pellets were resuspended in RIPA buffer [protease and phosphatase inhibitors and 1mM DTT were added] and then frozen at -80°C. From this point, all the procedures were performed at 4°C or in ice. Once thawed, cell lysates were resuspended every 15 minutes for 4 times and then sonicated 30 seconds with pulse [output approximately 10 watts. Then, samples were centrifugated at 13850 rcf for 10 minutes. Supernatants were collected and an equal volume of 20% SDS-6% DTT was added. The samples were incubated at 95°C for 5 minutes. Then, 5 volumes of MATF (Methanol, Acetone and Tributhyl phosphate, 1:12:1) were added and samples were incubated for 1h on a rotating wheel. The total proteins were finally precipitated by centrifugation at 12000 rcf for 15 minutes, the supernatants were eliminated and the protein pellets were dried for about 30 minutes at RT in a Savant SpeedVac apparatus. Each dried pellet was resuspended with 250 µl of 5% SDS in 50 mM Ammonium Bicarbonate [AMBIC]. After a brief centrifugation, 2 µl of each sample were processed to determine the protein concentration using the QuantiPro BCA Assay Kit [Sigma-Aldrich, St. Louis, Mo, USA]. Afterward, 20 mM DTT was added to 50 µg of total proteins for each sample and they were incubated at 95°C for 10 minutes. Once the samples were cooled to RT, Iodoacetamide was added to a final concentration of 40 mM and then the reaction mixtures were incubated for 30 minutes in the dark. Finally, orthophosphoric acid was added to a final concentration of 1,2%. The reduced and alkylated protein samples were loaded onto S-Trap mini columns, washed and then trypsin digested as suggested by the manufacturer (Protifi, Farmingdale NY, USA). The eluted mixtures were dried at RT. To perform mass spectrometry analysis, the desiccated tryptic digests were resuspended with 0.2% formic acid in water and analyzed by nano-UHPLC-MS/MS using an Ultimate 3000 chromatography system, equipped with a PepMap RSLC C18 EASY spray column [75 µm × 50 cm, 2 µm particle size] at a flow rate of 250 nl/min and a temperature of 60°C. The following mobile phase composition has been used: A] 0.1% v/v formic acid in water and B] 80% ACN, 20% H_2O and 0.08% v/v formic acid. A 105 min gradient was selected: 0.0-3.0 min isocratic 2% B; 3.0-7.0 min 7% B; 7.0-65.0 min 30% B; 65.0-78.0 min 45% B; 78.0-83.0 min 80% B; 83.0-85.0 isocratic 80% B; 85.0-85.1 2% B and finally 85.1-105.0 isocratic 2% B. After separation, the flow has been directly sent to an Easyspray source connected to a Q Exactive™ Plus Hybrid Quadrupole-Orbitrap™ mass spectrometer. The data were acquired in data-dependent mode, alternating between MS and MS/MS scans. The software Xcalibur [version 4.1, Thermo Scientific Instrument] has been used for operating the UHPLC/HR-MS. MS scans were acquired at a resolution of 70,000 between 200 and 2,000 m/z, with an automatic gain control [AGC] target of 3.0E6 and a maximum injection time [maxIT] of 100 ms. MS/MS spectra were acquired at a resolution of 17,500 with an AGC target of 1.0E5 and a maxIT of 50 ms. A quadrupole isolation window of 2.0 m/z was used, and HCD has been performed using 30 normalized collision energy [NCE]. The mass spectrometry proteomics data have been deposited to the ProteomeXchange Consortium via the PRIDE [20] partner repository with the dataset identifier PXD037657. (Reviewer account details, Username: reviewer_pxd037657@ebi.ac.uk, Password: ab7lZU5w). Data from mass spectrometer in *.raw format was processed with ProteomeDiscoverer® software version 2.4.1.15 (Thermo Scientific Instrument) for PMSs identification in MS/MS spectra, PMSs and protein quantification and for differential proteomics as explained in "Data Processing Protocol" paragraph

 doi:10.20944/preprints202304.0002.v1

at PXD037657 project. Peptide's abundances were normalized based on total peptide amount and scaled on all average. Proteins were quantified using IMP-apQuant node by summed abundances, pairwise ratio based and t-test background based. Significative differentially expressed proteins [DEPs] were choose for each group using a Log_2 Fold change > 2 and a $P<0.05$.

Electron microscopy

Wild type and Tz-res cell lines BT474, MDA-MD-361 and SKBR-3 were were seeded overnight on glass chamber slides (Lab-Tek 177380, Nalge Nunc int., Rochester, NY, USA). Cells were washed out in 0.1M cacodylate buffer and fixed in 0.1M cacodylate buffer containing 2.5% glutaraldehyde (Electron Microscopy Science, Hatfield, PA, USA), for 1 hour at RT. Samples were postfixed in osmium tetroxide for 2 hours and 1% uranyl acetate for 1 hour. Cells were next dehydrated through a graded ethanol series and flat embedded in resin (Poly-Bed; Polysciences, Inc., Warrington, PA, USA) for 24 hours at 60°C. Ultrathin sections [50 nm] were cut and stained with 5% uranyl acetate in 50% ethanol and observed with Hitachi 7800 electron microscope (Hitachi, Tokyo, Japan) [21]. Digital images were taken with a Megaview III camera and Radius 2.0 software (EMSIS, Muenster, Germany). Analysis of number and size of morphologically identified lipid droplets (LDs), were assessed in 10 cells for each condition. The diameter of each organelle was measured with the line tool of Radius 2.0 software (EMSIS, Muenster, Germany) and plotted as histograms ± SEM.

Statistical Analyses

Analyses was performed using Prism (GraphPad Software, La Jolla, CA, USA). We used the multiple unpaired t-test to evaluate cell proliferation differences. To measure cell survival, we used the unpaired t-test with Welch's correction. A Brown-Forsythe and Welch ANOVA test with a Dunnett's T3 multiple comparisons test was used to evaluate ERBB2 expression levels by FCM analysis. A t-test was performed to evaluate Lipid droplets (LDs)size, and number. Mean differences were considered statistically significant at $P < 0.05$.

3. Results

3.1. Generation and characterization of ERBB2+ Tz-R cell lines.

To obtain Tz-R cells, BT474, MDA-MD-36, and SKBR-3 were cultured and expanded in medium containing Tz at the initial concentration of 10 μg/ml progressively increased over about 6 months, to the final concentration of 160, 200, and 250 μg/ml for BT474, MDA-MD-361, and SKBR-3, respectively. Cells were routinely cultured in the Tz-containing medium for a further year before analysis. BT474, MDA-MB-361 and SKBR-3 Tz-R cells showed no statistical significant difference in survival rate after 72 h of treatment with 100 μg/ml Tz vs. controls while wt cells showed a statistically significant reduction corresponding to 58.2, 60.1, and 69.7 %, respectively, vs. controls (Figure 1).

Preprints (www.preprints.org) | NOT PEER-REVIEWED | Posted: 3 April 2023 doi:10.20944/preprints202304.0002.v1

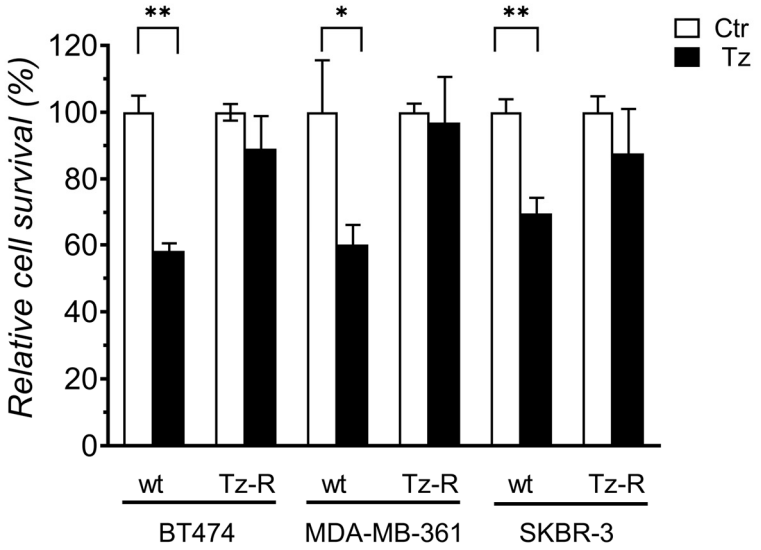

Figure 1. Cell survival analysis of ERBB2+ BCa cell lines treated with 10 μg/ml Tz compared with controls [Ctr]. *P*-values between each control and treated sample for each cell line are shown: $P<0.05$[*], $P<0.01$[**].

Microscopic analysis in bright field and phase contrast showed that SKBR-3 Tz-R respect to wt cells displayed a more homogeneous and typical epithelial phenotype with a large portion of the plasma-membrane involved in extended intercellular contacts. No major differences were observed instead between BT474 and MDA-MB-361 wt and Tz-R cells (Figure 2).

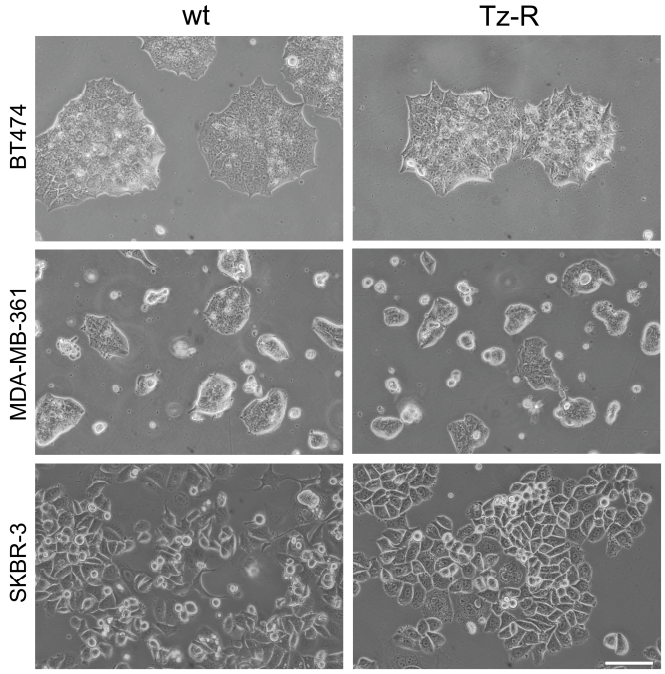

Figure 2. Phase-contrast images of ERBB2+ BCa wt and Tz-R cell lines used in this study. Scale bar=200 μm.

As previous report showed a reduced growth rate in Tz-R cell lines derived from gastric cancer [22], we investigated whether reduced proliferation was a character shared by all three our Tz-R cell

Preprints (www.preprints.org) | NOT PEER-REVIEWED | Posted: 3 April 2023 doi:10.20944/preprints202304.0002.v1

lines. In particular, we performed cell-growth curves by counting cells recovered from cultures at several time points after seeding. This analysis showed, instead, that a higher number of cells was significantly recovered from SKBR-3 Tz-R and MDA-MB-361 Tz-R in at the last two time points of the analysis than in wt cultures while no difference was observed between BT474 Tz-R and wt (Figure 3).

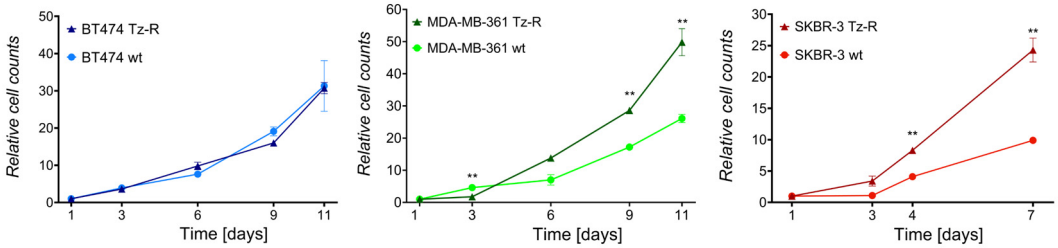

Figure 3. Growth curves of ERBB2+ BCa wt and Tz-R cell lines used in this study. Cell counts at each time point are reported as fold changes respect to those counted 1 day after seeding for each culture. Mean values and SD [indicated as vertical bars] are reported. Significant adjusted *P*-values are shown: $P<0.01$[**].

As mechanisms of ERBB2-targeted resistance have been associated to changes in the expression levels of several proteins belonging to different pathways such as ERBB receptors, RAS-MAPK, PI3K-AKT, PGR, and ER we have analyzed the expression levels of these along with other proteins related to masking mechanisms [23,24]. In particular, protein levels from whole cell lysates were obtained from proteomic analysis. Abundance ratio of protein expression levels in Tz-R vs wt cells found with high FDR confidence in samples from the cell lines used in the study are shown in Table S1. None of the listed markers were consistently modulated in all three Tz-R vs wt cells. Worth of note is that four proteins were found modulated with an abundance ratio with statistically significant adjusted P-values [$P<0.05$]. These were CDK6, EGFR, MUC1, and ERBB2. CDK6 was upregulated in Tz-R BT474 while EGFR and MUC1 were upregulated in Tz-R SKBR-3 cells. ERBB2 was found downregulated in Tz-R MDA-MB-361. As downregulation of ERBB2 after Tz therapy has been observed in vitro and in vivo and this may promote resistance toward Tz [16,25], we evaluated whether this mechanism was present in all our Tz-R cell models at the level of the plasma membrane [PM] where ERBB2 plays his main role. FCM analysis with the Tz antibody used to detect ERBB2, revealed that MDA-MB-361 Tz-R displayed a robust and statistically significant decrease in the levels of ERBB2 exposed on their PM. On the contrary, SKBR-3 Tz-R displayed a significant increase of surface-exposed ERBB2 while BT474 Tz-R cells showed only minor non-significant changes in ERBB2 PM levels respect to wt cells (Figure 4). Full statistical significance results of this FCM analysis are provided in Table S2.

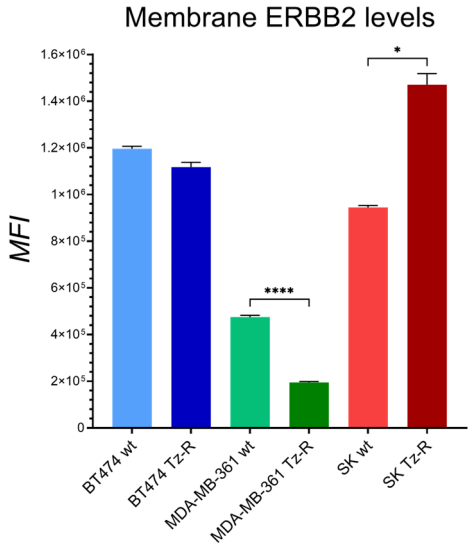

Preprints (www.preprints.org) | NOT PEER-REVIEWED | Posted: 3 April 2023 doi:10.20944/preprints202304.0002.v1

Figure 4. Plasma membrane ERBB2 median fluorescence intensity [MFI] expression levels in ERBB2+ BCa cell lines. All cell lines were first incubated with Tz and then with an anti-human Alexa 647 antibody. Only significant adjusted *P*-values between each wt and Tz-R cells belonging to the same cell line are shown: $P<0.05$[*], $P<0.0001$[****]. A complete list of the statistical analysis results is provided in Table S2.

3.2. Proteomic analysis of ERBB2+ and Tz-R cell lines reveals deregulation of lipid metabolism, organophosphate biosynthetic process, and macromolecule methylation.

To gain insight on the protein associated with the acquisition of Tz resistance, we used a proteomic and unbiased approach relying on high-resolution mass spectrometry on whole lysate of BT474, MDA-MB-361, and SKBR-3 wt and their counterpart Tz-R cells. This analysis was performed using 2 biological replicates and each replicate was run 2 times. Similar protein abundance was detected in each sample (Supplementary File 1). In particular, a range of 3141-3271 proteins with high FDR were identified in the three wt samples while 3021-3056 were identified in the three Tz-R samples. To reveal differences or similarities between the two conditions, wt and TZ-R, we performed a principal component analysis [PCA]. The PCA analysis showed that the proteins were separated in three main groups according to the cell line and that within each of these 3 main groups the TZ-R samples were separated from the wt ones (Figure 5A). An unsupervised hierarchical clustering analysis showed that the modulated proteins are clustered in three well defined groups, corresponding to the three cell lines, which is in agreement with the PCA analysis (Figure 5B).

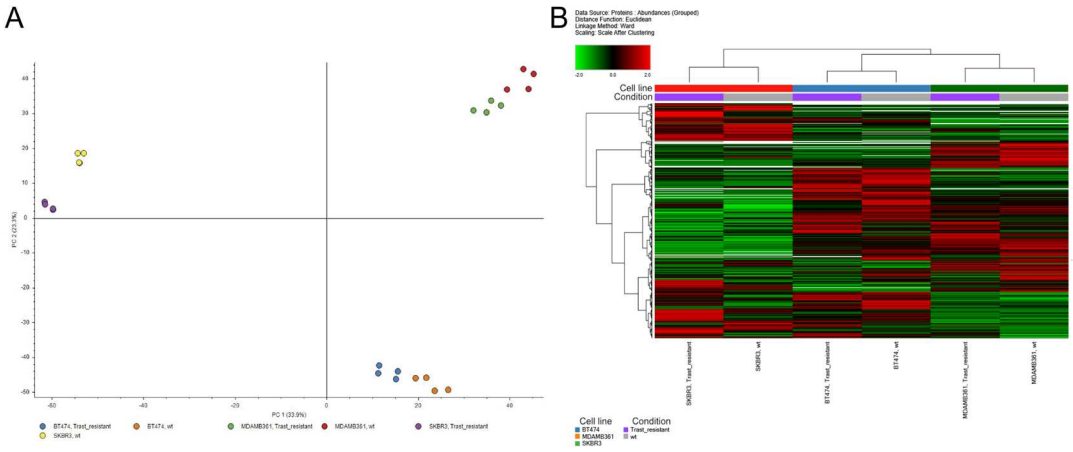

Figure 5. [A] Two-dimensional scatter plot of the principal component analysis of proteins expressed by wt and Tz-R [Trast_Resistant] ERBB2+ BCa cell lines used in this study. [B] Unsupervised hierarchical-clustered heatmap of identified DEPs. The amount of each protein in individual samples is represented by the color scheme in which red and green indicate high and low expression of proteins, respectively. Proteins are clustered into 3 groups according to their expression value, which correspond to the 3 main cell lines.

In particular, after excluding the IgG heavy chain of the Tz present in growth medium of Tz-R cells, and comparing the wt vs. TZ-R cell lines, we found 141 differentially expressed proteins [DEPs] in BT474, 138 in MDA-MB-361, and 220 in SKBR-3 (Figure 6).

Preprints (www.preprints.org) | NOT PEER-REVIEWED | Posted: 3 April 2023 doi:10.20944/preprints202304.0002.v1

Figure 6. Venn diagram representing DEPs in ERBB2+ BCa Tz-R vs wt cell lines. The number of DEPs proteins identified in each cell line is reported along with the number of those shared among them.

A list of all these DEPs is provided (Table S3). Interestingly, we observed that the three cell lines shared 10 DEPs. Among these, we noticed that 5 of these DEPs were undetectable in the three Tz-R models or downregulated vs. their wt counterpart (Upper 5 protein listed in Figure 7). However, study of the literature showed that these 10 common DEPs are associated to different cellular compartments and functions, which did not allow to infer a common biological process deregulated in the three Tz-R cell lines (Figure 7).

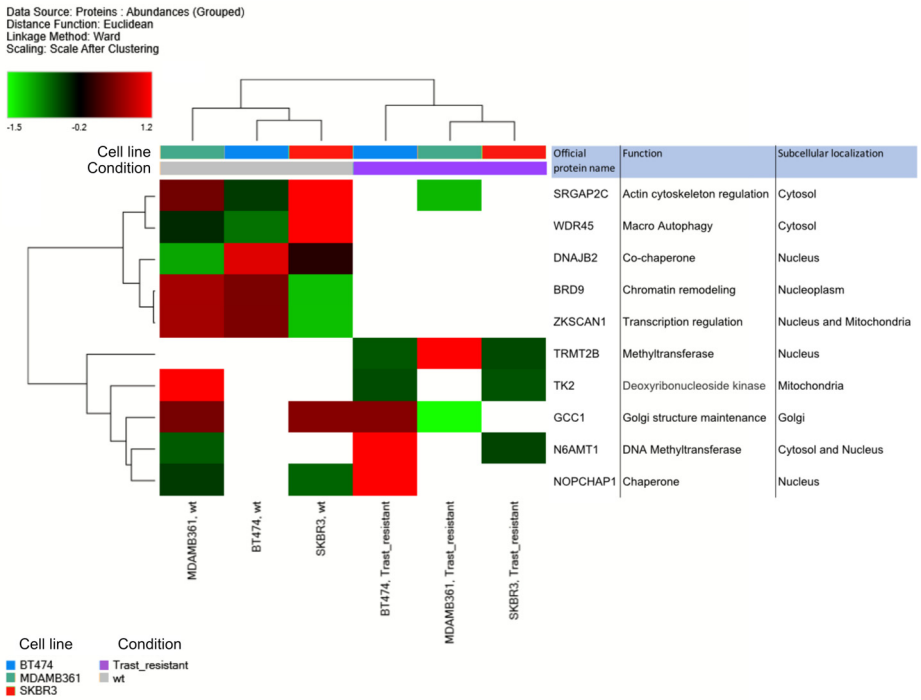

Figure 7. Unsupervised hierarchical-clustered heatmap of 10 DEPs that were find regulated by all three Tz resistant cell lines. The amount of each protein in individual samples is represented by the color scheme in which red and green indicate high and low expression of proteins, respectively. White boxes indicate expression level below the mass spectrometry detection threshold. Proteins are clustered into 2 main groups according to their expression value, which correspond to the 2 conditions: wt and Tz resistant cells. Official protein names, functions and subcellular localizations are indicated on the right.

Preprints (www.preprints.org) | NOT PEER-REVIEWED | Posted: 3 April 2023 doi:10.20944/preprints202304.0002.v1

To gain insights into biological processes deregulated in the Tz-R condition, we performed a pathway and process enrichment analysis submitting all the DEPs found in each of the three lines to the Database for Annotation, Visualization and Integrated Discovery [DAVID] tools, and to the Metascape resource, available at https://david.ncifcrf.gov and https://metascape.org, respectively. Using DAVID tools we found that DEPs in our Tz-R cell models were significantly associated to specific pathways included in the KEGG collection. Interestingly, metabolic pathways were an entry shared by the three lines (Table 1).

Table 1. Association of DEPs to pathways included in the KEGG collection and statistical significance as calculated by tools available at DAVID [https://david.ncifcrf.gov/tools.jsp]. Shared pathways are in italic.

BT474 wt vs. TzR			MDA-MB-361 wt vs TzR			SKBR-3 wt vs TzR		
KEGG Pathway	% of DE	P-Value	KEGG Pathway	% of DEPs	P-Value	KEGG Pathway	% of D	P-Value
Metabolic pathways	*18,6*	*5,00E-05*	Chronic myeloid leukemia	2,9	1,40E-02	*Metabolic pathways*	*28*	*7,00E-03*
Biosynthesis of cofactors	4,3	5,00E-03	TGF-beta signaling pathway	2,9	2,50E-02	Thyroid hormone signaling pathway	6	1,10E-02
			Metabolic pathways	*17*	*4,30E-02*	Glycerophospholipid metabolism	5	2,40E-02
			Proteoglycans in cancer	5	4,90E-02			

Metascape allowed us to define more specifically that metabolism of lipids reactome gene set, along with organophosphate biosynthetic process, and macromolecule methylation, were enriched and shared terms significantly associated to DEPs across the three cell lines (Table 2).

Table 2. Top 3 clusters with their representative enriched terrns [one per cluster]. Count is the number of DEPs with membership in the given gene ontology [GO] term. % is the percentage of all DEPs that are found in the given ontology term [only input proteins with at least one ontology term annotation are included in the calculation]. Log10[P] is the p-vatue in log base 10. Log10[q] is the multi-test adjusted p-value in log base 10. PATTERN shows the color code used for the protein Iists where the term is found statistically significant, i.e , the multiple colors indicate a pathway/process that is shared across the three DEP lists [Red-SKBR-3; Blue-BT474; Green-MDA-MB-361]. The analysis was performed by tools available at https://metascape.org.

PATTERN	GO	Category	Descrlptlon	Count	%	Log10(P)	Log10(q)
■ ■ ■	R-HSA-556833	Reactome Gene Sets	Metabolism of lipids	36	8,98	-10,5	-6,15
■ ■ ■	GO:0090407	GO Biological Processes	organophosphate biosynthetic process	28	6,98	-8,89	-4,84
■ ■ ■	GO:0043414	GO Biological Processes	macromolecule methylation	11	7,97	-7,18	-3,13

3.3. Electron microscopy revealed changes in lipid droplets content in Tz-R cells.

The results obtained from the proteomic analysis, prompted us to characterize the subcellular phenotype possibly associated with the deregulation of lipid metabolism in Tz-R cells. With this aim, we performed an ultrastructural examination of lipid droplets (LDs) in BT474, MDA-MB-361, and SKBR-3 wt and their counterpart Tz-R cells. EM analysis revealed that MDA-MB-361 and SKBR-3 Tz-R cells displayed a significant increase in the number of morphologically identified LDs with comparable size, while in BT474 Tz-R cells this increase was present but not significant. However, BT474 Tz-R cells showed a significant reduction of LDs size (Figure 8).

Preprints (www.preprints.org) | NOT PEER-REVIEWED | Posted: 3 April 2023 doi:10.20944/preprints202304.0002.v1

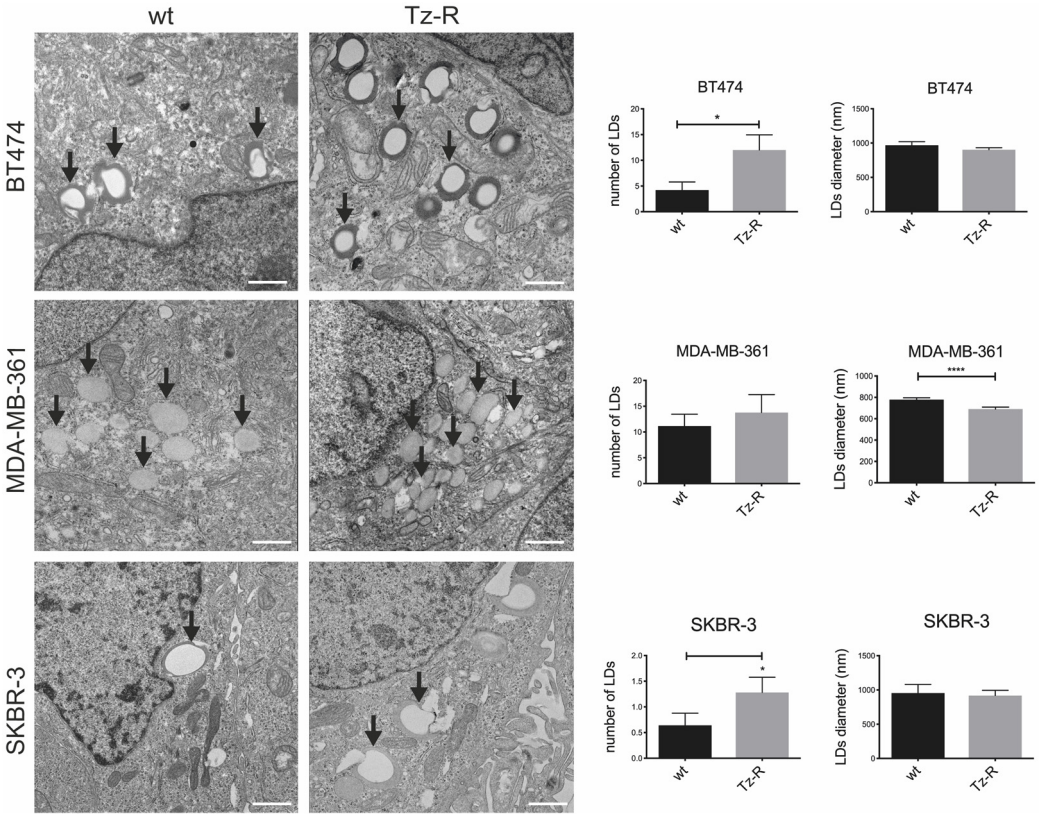

Figure 8. Representative TEM images of ERBB2+ BCa wt and Tz-R cell lines. Lipid droplets [LDs] were morphologically identified [black arrows]. Histograms show the LDs number and diameter measured for each experimental condition. For this analysis, 10 whole cells were scored and measured for LDs with Radius 2.0 imaging software. $P = 0.023$ [*] for SKBR-3, $P = 0.032$ [*] for BT474 [LDs number] and $P < 0.0001$[****] for MDA-MB-361 [LDs diameter], respectively. Scale bars: 1 μm.

4. Discussion

Trastuzumab resistance remains a challenging occurrence in BCa patients' managements and deserves further study to be better understood. Changes elicited by Tz in the cancer cells during treatment may have a major role in treated patients with reduced immune response due to chemotherapeutics associated to Tz. In vitro study may help in their identification. The aim of this study was to highlight a possible common mechanism at the base of trastuzumab resistance in ERBB2+ BCa cell lines. Our unbiased study points toward a metabolic reprogramming contributing to Tz resistant in ERBB2+ BCa cells derived from cell lines with different receptor status and sensitivity to Tz. In particular, we used the widely available cell lines BT474, MDA-MB-361, and SKBR-3 and adapted them to grow in medium containing Tz concentration up to about 10 times those found in serum of treated patients.

Phase-contrast microscopy analysis showed that Tz resistance in the three cell lines does not result in common changes in cell morphology respect to the wt counterparts. Growth curves of our cell lines showed that in our models of Tz-R cells higher proliferation were observed in MDA-MD361 and SKBR-3 Tz-R cells but not in BT474 Tz-R cells. Our results is not in agreement with a previous study but the reason could be due to the different ERBB2+ tumor type studied [22]. According to proliferation analysis, ERBB2 expression analysis by FCM also showed a non-consistent modulation of its levels on the PM among our Tz-R cells. This result ruled out receptor downmodulation as a common mechanism associated to Tz resistance in our models. Similarly, proteomic data also ruled out in our models a common deregulation of proteins belonging to pathways related to ERBB2 targeted therapy resistance such as ERBB receptors, RAS-MAPK, PI3K-AKT, PGR, and ER or related to ERBB2 masking mechanisms. Proteomic analysis data, and in particular PCA, showed that each Tz-R cell line was closely related to the original wt line and that the three cell lines could be well

separated from each other. In details, we found that about 138-220 proteins were differently regulated in the Tz-R cells respect to each wt counterpart. This indicated that using an arbitrary Log_2 Fold change > 2 in protein expression levels, a small set of differentially expressed proteins was associated to the Tz resistant status. Among these DEPs, we found 10 proteins shared among the three models and hierarchical clustering clearly showed a subset of 5 of these DEPs that were downregulated or altogether undetected in the Tz-R cell lines. We found of particular interest that SRGAP2C and WDR45 were included in this 5 DEPs subset. Our observation, along with previous data showing that these two proteins are positive prognostic markers when overexpressed in cancer [26,27], suggests that the loss of functions associated to these 5 DEPs may play a role in promoting a more aggressive character to Tz resistant cells. The opposite may apply to TRMT2B which was, instead, undetectable in all our ERBB2+ BCa wt cells. We also found that 4 proteins among these 10 DEPs were not consistently regulated in the three cell models by Tz resistance: TK2, GCC1, N6AMT1, and NOPCHAP1. Overall, our data prompt further studies to better establish the relationship of these 10 common DEPs with Tz resistance. As expected by the size of the 10-protein set shared among the Tz-R cells, the bioinformatic tools that we used could not point to common biological processes associated with it. However, when we analyzed the DEPs in each cell line, we found that a common biological process was associated with statistical significance to Tz resistance: metabolic pathways. Furthermore, we could establish that, in particular, lipid metabolism, organophosphate biosynthetic process, and macromolecule methylation were pathways associated to Tz resistance in all our three cell line models.

Lipid droplets are storage organelles pivotal for lipid and energy homeostasis. Altered lipid metabolism mediates drug resistance to small molecule inhibitors of HER2 kinase in breast cancer, raising a link between kinase signaling reprogramming and lipid metabolism [28]. Indeed, we observed significant changes in LDs size or number within the three Tz resistant cell lines by electron microscopy pointing to a remodeling of their lipid production and or accumulation compared to wt. Our results are in line with previous reports suggesting that metabolic rewiring may contribute to Tz resistance. In particular, previous studies showed that fatty acid metabolism, membrane lipid rafts, and ERBB2 pathogenesis have close relationships [16] and that Tz increases lipogenesis via FAS promoter [29]. Furthermore, a previous study showed that lapatinib-resistant cells undergo a CD63-mediated rewiring of the lipid metabolism [30]. Concerning the methylation of macromolecules, it is interesting to note that HSD17B4 methylation was identified as a predictive response marker to HER2-directed therapy in ERBB2+ BCa [31] and that genes involved in cancer-related pathways were frequently affected by epigenetic alterations in HER2-positive breast cancer [32]. Even more relevant is that epigenetic silencing of TGFBI was found to confer resistance to trastuzumab in human breast cancer [33]. Therefore, our results further underline the importance of methylation of macromolecules in the development of Tz resistance.

5. Conclusions

Our data strongly support the hypothesis that complex metabolic adaptation, including lipid metabolism, protein phosphorylation, and possibly chromatin remodeling, may fuel Tz resistance. Our study also identified a common set of 10 DEPs in all three TZ-resistant cell lines that may provide novel targets for therapeutic intervention.

6. Patents

Not applicable.

Supplementary Materials: The following supporting information can be downloaded at the website of this paper posted on Preprints.org. Figure S1: Box-and-whisker plot showing protein abundance levels in each cell line sample as determined by high resolution mass spectrometry analysis; Table S1: Proteins relevant for resistance to ERBB2-targeted therapies in BCa found with high FDR confidence in samples from the cell lines used in the study; Table S2: Results of the Brown-Forsythe and Welch ANOVA test with a Dunnett's T3 multiple comparisons test of the ERBB2 expressed on the plasma membrane of the cell lines used in the study; Table S3: List of differentially expressed proteins (DEPS) in BT474, MDA-MB-361, and SKBR-3Tz-R vs. wt cells.

Author Contributions: Conceptualization, Katia Cortese and Patrizio Castagnola; Data curation, Gabriela Coronel Vargas and Erika Iervasi; Formal analysis, Katia Cortese and Patrizio Castagnola; Funding acquisition, Katia Cortese and Patrizio Castagnola; Investigation, Marco Ponassi, Aldo Profumo, Gabriela Coronel Vargas, Erika Iervasi, Grazia Bellese, Sara Tavella, Maria Cristina Gagliani, Katia Cortese, and Patrizio Castagnola; Methodology, Marco Ponassi, Aldo Profumo, Gabriela Coronel Vargas, Erika Iervasi, Maria Cristina Gagliani, Katia Cortese, and Patrizio Castagnola; Supervision, Katia Cortese and Patrizio Castagnola; Writing – original draft, Katia Cortese and Patrizio Castagnola; Writing – review & editing, Katia Cortese and Patrizio Castagnola. All authors have read and agreed to the published version of the manuscript.

Funding: This research was funded by grants from Italian Ministry of Health (Ricerca Corrente) to PC and by University of Genova research grant funding (FRA, Fondi Ricerca Ateneo, 100008-2022-KC-FRA_ANATOMIA) to KC.

Data Availability Statement: The authors confirm that the data supporting the findings of this study are available within the article and/or its supplementary materials.

Acknowledgments: We thank the University of Genoa for funding the acquisition of the HITACHI 120kV TEM microscope HT7800, (Grant D.R. 3404, Heavy Equipment).

Conflicts of Interest: The authors declare no conflict of interest.

References

1. Slamon DJ, Clark GM, Wong SG, Levin WJ, Ullrich A, McGuire WL. Human breast cancer: correlation of relapse and survival with amplification of the HER-2/neu oncogene. Science. 1987;235:177–82.
2. Slamon DJ, Godolphin W, Jones LA, Holt JA, Wong SG, Keith DE, et al. Studies of the HER-2/neu proto-oncogene in human breast and ovarian cancer. Science. 1989;244:707–12.
3. Wang Z. ErbB Receptors and Cancer. Methods Mol Biol. 2017;1652:3–35.
4. Braicu C, Buse M, Busuioc C, Drula R, Gulei D, Raduly L, et al. A Comprehensive Review on MAPK: A Promising Therapeutic Target in Cancer. Cancers [Basel]. 2019;11:E1618.
5. Revathidevi S, Munirajan AK. Akt in cancer: Mediator and more. Semin Cancer Biol. 2019;59:80–91.
6. Greenberg PA, Hortobagyi GN, Smith TL, Ziegler LD, Frye DK, Buzdar AU. Long-term follow-up of patients with complete remission following combination chemotherapy for metastatic breast cancer. J Clin Oncol. 1996;14:2197–205.
7. Vogel CL, Cobleigh MA, Tripathy D, Gutheil JC, Harris LN, Fehrenbacher L, et al. Efficacy and safety of trastuzumab as a single agent in first-line treatment of HER2-overexpressing metastatic breast cancer. J Clin Oncol. 2002;20:719–26.
8. Cortés J, Kim S-B, Chung W-P, Im S-A, Park YH, Hegg R, et al. Trastuzumab Deruxtecan versus Trastuzumab Emtansine for Breast Cancer. N Engl J Med. 2022;386:1143–54.
9. Lane HA, Motoyama AB, Beuvink I, Hynes NE. Modulation of p27/Cdk2 complex formation through 4D5-mediated inhibition of HER2 receptor signaling. Ann Oncol. 2001;12 Suppl 1:S21-22.
10. Denny EC, Kane SE. t-Darpp Promotes Enhanced EGFR Activation and New Drug Synergies in Her2-Positive Breast Cancer Cells. PLoS One. 2015;10:e0132267.
11. Maadi H, Soheilifar MH, Choi W-S, Moshtaghian A, Wang Z. Trastuzumab Mechanism of Action; 20 Years of Research to Unravel a Dilemma. Cancers [Basel]. 2021;13:3540.
12. Moasser MM. Inactivating Amplified HER2: Challenges, Dilemmas, and Future Directions. Cancer Res. 2022;82:2811–20.
13. D'Alesio C, Bellese G, Gagliani MC, Lechiara A, Dameri M, Grasselli E, et al. The chromodomain helicase CHD4 regulates ERBB2 signaling pathway and autophagy in ERBB2+ breast cancer cells. Biology Open. 2019;bio.038323.
14. Nagata Y, Lan K-H, Zhou X, Tan M, Esteva FJ, Sahin AA, et al. PTEN activation contributes to tumor inhibition by trastuzumab, and loss of PTEN predicts trastuzumab resistance in patients. Cancer Cell. 2004;6:117–27.
15. Kreutzfeldt J, Rozeboom B, Dey N, De P. The trastuzumab era: current and upcoming targeted HER2+ breast cancer therapies. Am J Cancer Res. 2020;10:1045–67.
16. Vivekanandhan S, Knutson KL. Resistance to Trastuzumab. Cancers [Basel]. 2022;14:5115.
17. Dai X, Cheng H, Bai Z, Li J. Breast Cancer Cell Line Classification and Its Relevance with Breast Tumor Subtyping. J Cancer. 2017;8:3131–41.

18. Narayan M, Wilken JA, Harris LN, Baron AT, Kimbler KD, Maihle NJ. Trastuzumab-induced HER reprogramming in "resistant" breast carcinoma cells. Cancer Res. 2009;69:2191–4.
19. Cardinali B, Lunardi G, Millo E, Armirotti A, Damonte G, Profumo A, et al. Trastuzumab quantification in serum: a new, rapid, robust ELISA assay based on a mimetic peptide that specifically recognizes trastuzumab. Anal Bioanal Chem. 2014;406:4557–61.
20. Perez-Riverol Y, Bai J, Bandla C, García-Seisdedos D, Hewapathirana S, Kamatchinathan S, et al. The PRIDE database resources in 2022: a hub for mass spectrometry-based proteomics evidences. Nucleic Acids Res. 2022;50:D543–52.
21. D'Alesio C, Bellese G, Gagliani MC, Aiello C, Grasselli E, Marcocci G, et al. Cooperative antitumor activities of carnosic acid and Trastuzumab in ERBB2+ breast cancer cells. J Exp Clin Cancer Res. 2017;36:154.
22. Zuo Q, Liu J, Zhang J, Wu M, Guo L, Liao W. Development of trastuzumab-resistant human gastric carcinoma cell lines and mechanisms of drug resistance. Sci Rep. 2015;5:11634.
23. Swain SM, Shastry M, Hamilton E. Targeting HER2-positive breast cancer: advances and future directions. Nat Rev Drug Discov. 2023;22:101–26.
24. Menyhárt O, Santarpia L, Győrffy B. A Comprehensive Outline of Trastuzumab Resistance Biomarkers in HER2 Overexpressing Breast Cancer. Curr Cancer Drug Targets. 2015;15:665–83.
25. Ignatov T, Gorbunow F, Eggemann H, Ortmann O, Ignatov A. Loss of HER2 after HER2-targeted treatment. Breast Cancer Res Treat. 2019;175:401–8.
26. Marko TA, Shamsan GA, Edwards EN, Hazelton PE, Rathe SK, Cornax I, et al. Slit-Robo GTPase-Activating Protein 2 as a metastasis suppressor in osteosarcoma. Sci Rep. 2016;6:39059.
27. Fei H, Chen X. A Novel Autophagy-Related Prognostic Risk Model and a Nomogram for Survival Prediction of Oral Cancer Patients. Biomed Res Int. 2022;2022:2067540.
28. Feng WW, Kurokawa M. Lipid metabolic reprogramming as an emerging mechanism of resistance to kinase inhibitors in breast cancer. CDR [Internet]. 2019 [cited 2023 Jan 13]; Available from: https://cdrjournal.com/article/view/3303
29. Menendez JA, Vellon L, Mehmi I, Oza BP, Ropero S, Colomer R, et al. Inhibition of fatty acid synthase [FAS] suppresses *HER2/neu* [*erb* B-2] oncogene overexpression in cancer cells. Proc Natl Acad Sci USA. 2004;101:10715–20.
30. Feng WW, Wilkins O, Bang S, Ung M, Li J, An J, et al. CD36-Mediated Metabolic Rewiring of Breast Cancer Cells Promotes Resistance to HER2-Targeted Therapies. Cell Rep. 2019;29:3405-3420.e5.
31. Yamashita S, Hattori N, Fujii S, Yamaguchi T, Takahashi M, Hozumi Y, et al. Multi-omics analyses identify HSD17B4 methylation-silencing as a predictive and response marker of HER2-positive breast cancer to HER2-directed therapy. Sci Rep. 2020;10:15530.
32. Yamaguchi T, Mukai H, Yamashita S, Fujii S, Ushijima T. Comprehensive DNA Methylation and Extensive Mutation Analyses of HER2-Positive Breast Cancer. Oncology. 2015;88:377–84.
33. Palomeras S, Diaz-Lagares Á, Viñas G, Setien F, Ferreira HJ, Oliveras G, et al. Epigenetic silencing of TGFBI confers resistance to trastuzumab in human breast cancer. Breast Cancer Res. 2019;21:79.